

This is the peer reviewed version of the following article: Yin, M. J., Yao, M., Gao, S., Zhang, A. P., Tam, H. Y., & Wai, P. K. A. (2016). Rapid 3D patterning of poly (acrylic acid) ionic hydrogel for miniature pH sensors. *Advanced Materials*, 28(7), 1394-1399, which has been published in final form at <https://doi.org/10.1002/adma.201504021>. This article may be used for non-commercial purposes in accordance with Wiley Terms and Conditions for Use of Self-Archived Versions. This article may not be enhanced, enriched or otherwise transformed into a derivative work, without express permission from Wiley or by statutory rights under applicable legislation. Copyright notices must not be removed, obscured or modified. The article must be linked to Wiley's version of record on Wiley Online Library and any embedding, framing or otherwise making available the article or pages thereof by third parties from platforms, services and websites other than Wiley Online Library must be prohibited.

Rapid 3D Patterning of Poly(acrylic acid) Ionic Hydrogel for Miniature pH Sensors

*Ming-jie Yin^a, Mian Yao^{a,b}, Shaorui Gao^a, A. Ping Zhang^{*a}, Hwa-yaw Tam^a, and Ping-kong A. Wai^b*

[a] Mr. M. J. Yin, Mr. M. Yao, Dr. S. Gao, Dr. A. P. Zhang, Prof. H. Y. Tam
Photonics Research Center, Department of Electrical Engineering, The Hong Kong Polytechnic University, Hong Kong SAR, China
E-mail: azhang@polyu.edu.hk

[b] Mr. M. Yao, Prof. P. K. A. Wai
Photonics Research Center, Department of Electronic and Information Engineering, The Hong Kong Polytechnic University, Hong Kong SAR, China

Keywords: PAA ionic hydrogel, photopolymerization, optical stereolithography, optical biosensor, pH sensor.

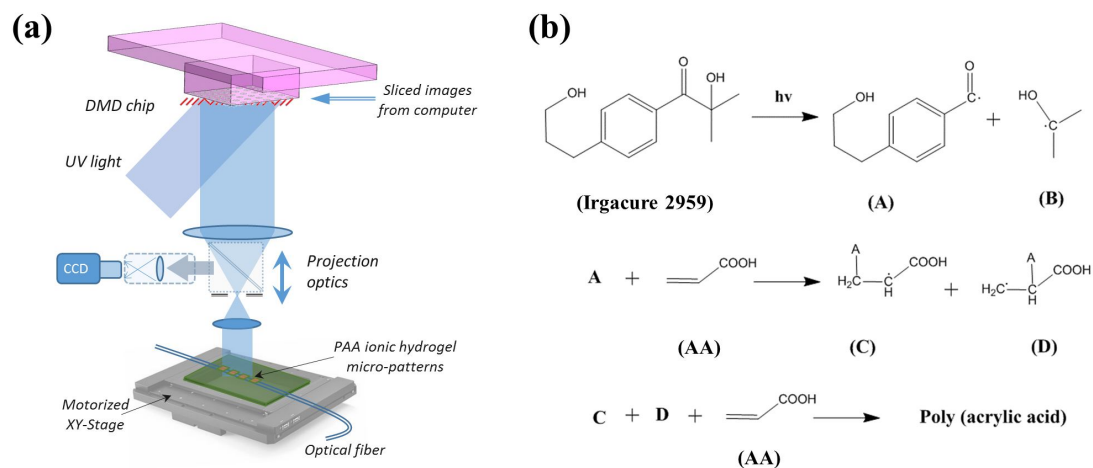
Ionic hydrogel is a kind of highly ionic conductive hydrophilic polymer containing cationic or anionic groups. As its hydrophilicity depends on the density of charged groups, ionic hydrogel is a stimuli-responsive gel that can reversibly swell/deswell according to the change of surrounding conditions,^[1] including ions, pH, organic solvent, light, electric field, temperature, and humidity. Among various ionic hydrogels, poly(acrylic acid) (PAA) has attracted remarkable interests due to its superior biocompatibility^[1d-1g, 2] as well as its perfect water absorptivity and good thin-film formability.^[2c, 2e, 2h, 2j] Moreover, the high density of carboxylic acids makes it suitable for physical and chemical modification to form bio-functional surfaces,^[2c] and thus, PAA has great potential to be deployed in rapidly emerging fields, such as tissue engineering, protein immobilization, biosensors and biomedical devices.^[1g, 2b, 2j, 2n, 3]

An essential step in advancing the development to fully utilize the superior properties of PAA ionic hydrogels in sensors is rapid prototyping using fast patterning technique to make fine and complicated microstructures. There have been demonstrations of several techniques to pattern PAA ionic hydrogels, including microcontact printing,^[2f, 4] ion beam lithography,^{[2e,}

^{2i, 5]} micromolding,^[2h, 6] evaporation-induced self-assembly,^[7] wet etching^[8] and photomask-based lithography.^[2c, 9] However, most of these techniques are time-consuming or require fastidious processing condition. Moreover, none of them can be used to fabricate 3D PAA microstructures and thus would limit the applications of PAA ionic hydrogels in e.g. mimicking the extracellular microenvironments and fabricating biosensors.^[10]

Recently, we have demonstrated a dynamic optical projection stereolithography (DOPsL) to rapidly fabricate 3D hydrogel scaffolds for tissue engineering.^[11] However, such an optical exposure technology works in a free-running manner and is not able to process hydrogel adaptive to substrate conditions. Thus, it still has considerable limitations on the fabrication of hydrogel based devices, in which a much-demanded need is to directly print hydrogel on a very small target or a micropatterned substrate to functionalize the device or modify its chemical properties. In this paper, we present an optical maskless stereolithography (OMsL) technology with enhanced features of *in-situ* microfabrication and large-area patterning. Specifically, optical imaging technology is integrated to visualise the optical exposure platform allowing *in-situ* patterning hydrogel on a very small area of target; a seamless pattern-stitching technique is developed for processing large-area microstructures and devices. In particular, we will demonstrate that PAA ionic hydrogel can be printed with high precision even on the surface of a tapered optical microfiber with diameter of 30 μm to develop an ultrasensitive fiber-optic pH sensor.

Scheme 1 shows the schematic diagram of OMsL technology and the photopolymerization process for acrylic acid (AA) initiated by Irgacure 2959. In the OMsL platform, a UV grade digital-mirror device (DMD) is used as a high-speed spatial light modulator for optical pattern generation. With an in-house developed control software, the light beam from a high-power UV source (with the wavelength of 365 nm) is modulated into an optical pattern with a million pixels in accordance with the image data from the control computer, and projected on the polymeric material for patterning microstructures. In order to



Scheme 1. (a) Schematic diagram of the OMsL system: UV light illuminates the DMD chip, and the generated optical pattern is projected on the photosensitive polymer to fabricate microstructures. (b) Reaction process for the photopolymerization of AA in the presence of photoinitiator.

in-situ pattern the polymeric material on a target area, a CCD camera based machine vision module was integrated together with a visible light based illumination system. A photo of the OMsL setup is shown in Figure S1 (a). Compared with other well-known maskless lithography technologies, e.g. scanning electron-beam lithography, two-photon polymerization lithography, this optical maskless exposure technology promises a much higher speed of patterning owing to its fast image projection capabilities.^[11]

Figure 1 shows some PAA microstructure images taken with a laser scanning confocal microscope. These microstructures were rapidly fabricated within 10 to 20 s. In order to shorten exposure time, the AA solution was heated before optical exposure process. Experimental results reveal that such a prepolymerization process not only expedites the photopolymerization process, but also improves the quality of the fabricated micropatterns. Figure 1 (a), (b), and (c) show three examples of 2D microstructures, i.e. a lattice grid, a honeycomb pattern, and the logo of our university, respectively. The surfaces of all the patterned microstructures are very smooth. The line widths of the three patterns are 6, 50, and 200 μm , respectively. Due to the inherent water-absorption property of hydrogel, the joint points of thick microstructure appear slightly swell, as shown in Figure 1 (c). The results

indicate that the lithography process is very promising to fabricate PAA microdevices with different feature sizes. The lateral and depth resolutions of the platform for patterning PAA are around 4.8 and 0.2 μm , respectively, see Figure S2. More details of the geometric parameters of the fabricated PAA micropatterns are presented in Figure S3 and Figure S4.

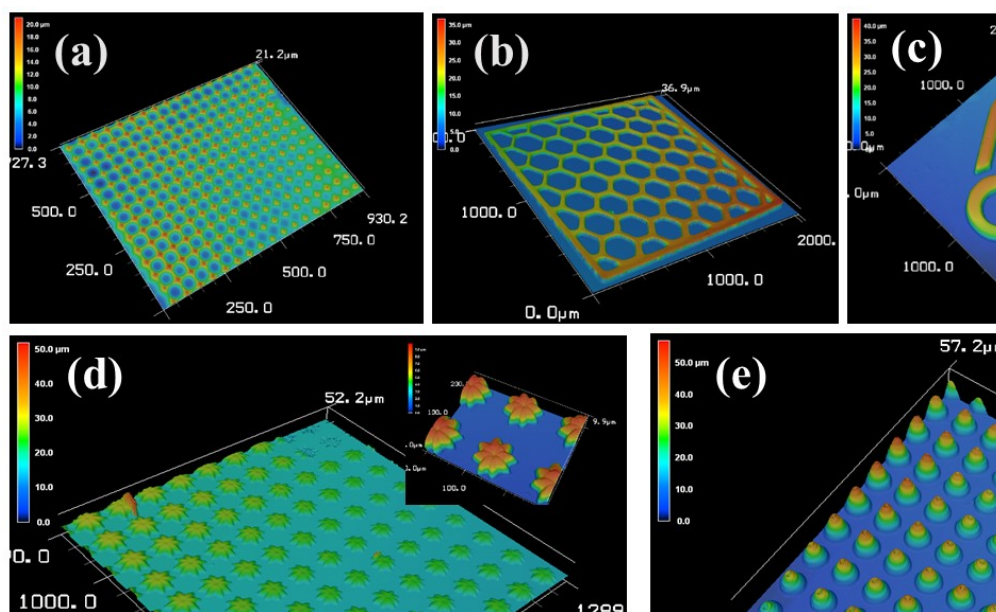


Figure 1. Laser scanning confocal images of the 3D patterned microstructures of PAA ionic hydrogels: (a) lattice grid, (b) honeycomb pattern, (c) PolyU logo, (d) flower-like microstructure, and (e) Hanoi-tower microarray.

Complex 3D PAA microstructures can also be fabricated by the OMsL technique through a layer-by-layer photopolymerization process, as shown in Figure S1 (b). Figure 1 (d) and (e) show the 3D printed flower-like microstructures and Hanoi-tower microarray, respectively. Compared with 2D microstructures, 3D microstructures need longer exposure time (around 30 s). The flower-like microstructure contains 8 petals, and its height gradually decreases from the center. The diameter of the 3D flower microstructure is 75 μm . The Hanoi-tower microstructures compose of 5 concentric rings with graded heights, and the size is 200 μm . These results indicate that the OMsL technology is able to fabricate various 3D PAA microstructures.

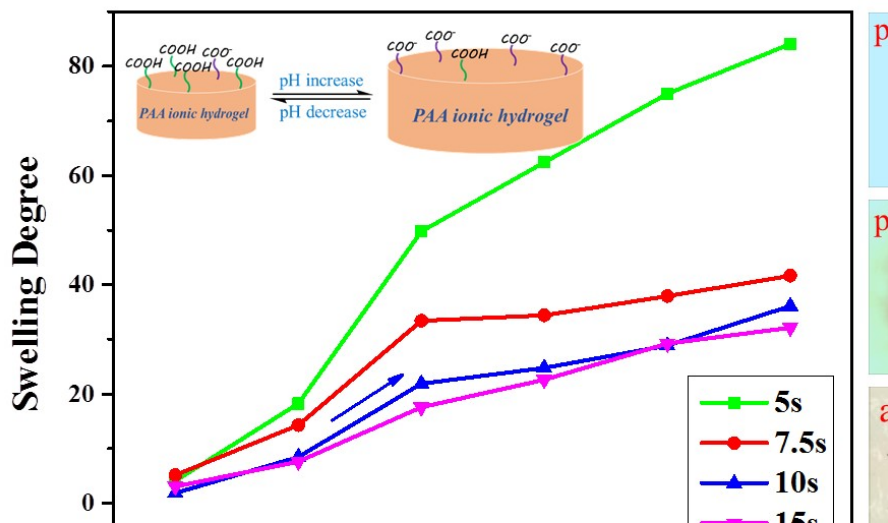


Figure 2. Swelling degree of PAA ionic hydrogel with increasing pH. The inset shows the swelling of PAA ionic hydrogel due to the pH induced change from $-\text{COOH}$ to $-\text{COO}^-$ group. Microscopic images of discoid PAA micropattern in different conditions (from bottom to top): in air; immersed sequentially into pH=2 and pH=4 solutions after 2 hours (scale bar: 250 μm).

To study the pH responsive behaviors of PAA ionic hydrogels, four discoid PAA micropatterns with different exposure strengths were prepared by using the OMsL setup. The exposure times used for photopolymerization of the four PAA micropatterns are 5.0, 7.5, 10.0, and 15.0 s, respectively. These PAA micropatterns are then immersed into different pH solutions for 2 hours. The swelling degree was determined by using the ratio of the mass of the hydrogel in the swollen and dried states based on gravimetric method. One can see from **Figure 2** that the PAA ionic hydrogel micropatterns swell with pH values from 2 to 7. The microscopic images of PAA micropatterns in air and in pH=2 and pH=4 solutions are shown on the right side of Figure 2. The dependence of the swelling degree with pH is shown in the inset of Figure 2. When increasing pH, the $-\text{COOH}$ group of PAA will be deprotonated to become $-\text{COO}^-$ group, and thus the hydrophilicity of PAA ionic hydrogels will be enhanced.^[1d, 1f] Moreover, PAA micropatterns irradiated with different exposure dose exhibit different swelling degrees. The PAA micropattern fabricated with shorter irradiation time swells more significantly than that under longer irradiation time. This phenomenon can be

attributed to the different molecular weights of PAAs resulted in diverse exposure times.^[12] The molecular weight of PAA micropattern fabricated in shorter exposure time is smaller, and so its hydrophilicity is more significant.^[13] It is noteworthy that there is no significant difference for PAA micropatterns irradiated for 10 and 15 s. It means that the molecular weight of the PAA micropattern irradiated for 10 s has become comparatively large, and longer-time irradiation will not lead to significant change of PAA molecular weight.

The 3D patterning technology and the distinctive pH responsive characteristics render the PAA ionic hydrogel a very promising material for microdevice and sensor applications. **Figure 3** (a) shows the schematic design of a periodic PAA micropads forming a long-period grating (PAA-LPG) as a miniature optical pH sensor. A standard single-mode optical fiber with diameter of 125 μm is tapered into a microfiber with diameter of $\sim 30 \mu\text{m}$ to enhance the

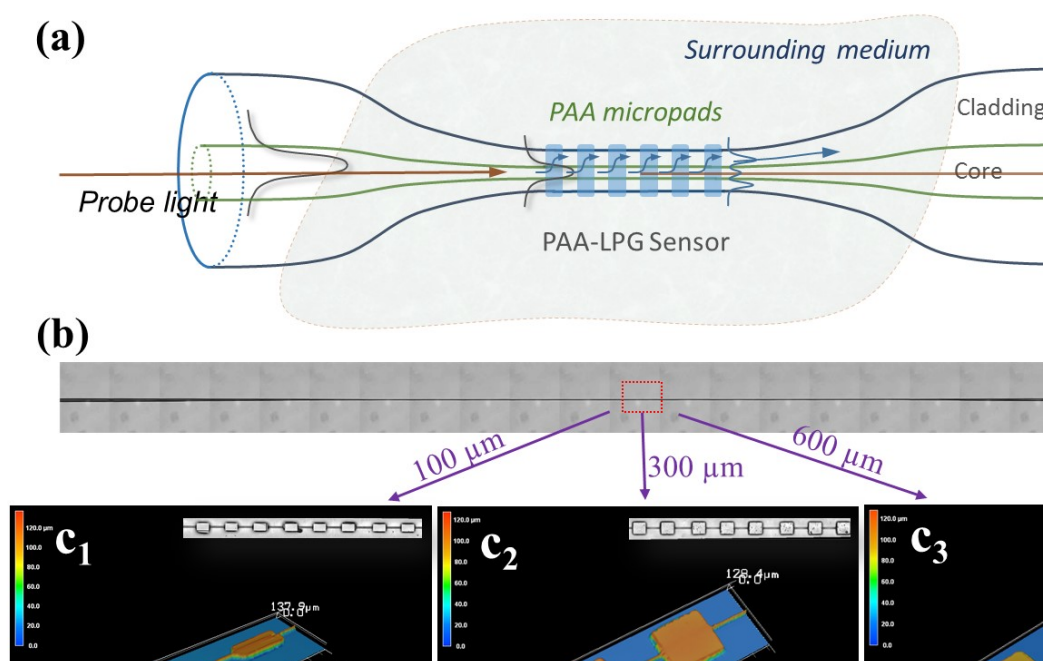


Figure 3. (a) Schematic design of a microfiber pH sensor based on micropatterned PAA ionic hydrogel. (b) Optical microscopic image of a tapered optical fiber with a diameter of 30 μm . (c) Confocal microscopic images of three kinds of PAA micropads of different sizes patterned to encapsulate the microfiber. The sizes of micropads of (c_1), (c_2), and (c_3) are 325 $\mu\text{m} \times 100 \mu\text{m}$, 325 $\mu\text{m} \times 300 \mu\text{m}$, and 325 $\mu\text{m} \times 600 \mu\text{m}$, respectively. The insets are the photos taken by optical microscope.

overlapping between the fundamental guided mode and cladding modes, and also the evanescent field of cladding modes. PAA ionic hydrogel is then patterned into a series of periodical micropads on the surface of the microfiber. Since photopolymerization process causes shrinkage in polymer, PAA micropads will act as “hoops” and apply a periodic strain modulation on the microfiber.^[14] Thanks to the enhanced overlapping between the fundamental guided mode and cladding modes, such a periodic strain modulation will cause a resonant scattering phenomena in the microfiber, and induce a coupling from the fundamental guided mode to a specific cladding mode at the resonant wavelength.

Figure 3 (b) shows the microscopic image of an optical microfiber tapered from a standard single-mode fiber. The fabricated microfiber was mounted on a glass slide and then dropped with PAA ionic hydrogel for patterning process, as shown in Figure S1 (c). Figure 3 (c₁ – c₃) are the confocal microscopic images of three examples of PAA micropads patterned on a microfiber. Experimental conditions were kept the same so as to obtain PAA micropads with the same thickness, and the irradiation time was chosen to 10 s according to the test data presented in Figure 2. In order to properly excite the resonant scattering of cladding modes at the wavelength of around 1430 nm, the grating pitch of LPGs has been chosen to be 650 μm . One can see that the PAA ionic hydrogel was precisely patterned to enclose small lengths of the tapered microfiber along the central line of micropattern. Both the size and pitch of PAA micropads are very uniform. It indicates that the OMsL technology is able to pattern PAA ionic hydrogel with high resolution to fabricate micro-structured devices.

For such a PAA-LPG device, its decisive factors in spectral characteristics as well as sensing performance are duty cycle and lateral width. Duty cycle not only determines the effective amplitude of the grating, but also governs the space between two PAA micropads for swelling actions; the lateral width of PAA micropads influences the absolute magnitude of the applied strain and thus determines resonant strength. For ease of description, the PAA-LPG

device is labelled as LPG- X - Y where the duty cycle of the grating is X and the lateral width of PAA micropad is Y in the sections below.

Figure 4 shows the measured transmission spectra of the 20-mm long PAA-LPGs with different lateral widths of PAA micropads. A broadband light source and an optical spectrum analyzer (OSA) were used in the measurement. One can see that the LPG resonant peaks become deeper with increment of the lateral width of PAA micropads, indicating that the coupling strength is enhanced. Meanwhile, the central resonant wavelength blue shifted slightly. It can be explained that the strain applied on the microfiber increased with the size of the PAA micropads. The induced change of the effective index of the cladding mode is larger than that of the fundamental guided mode.^[15]

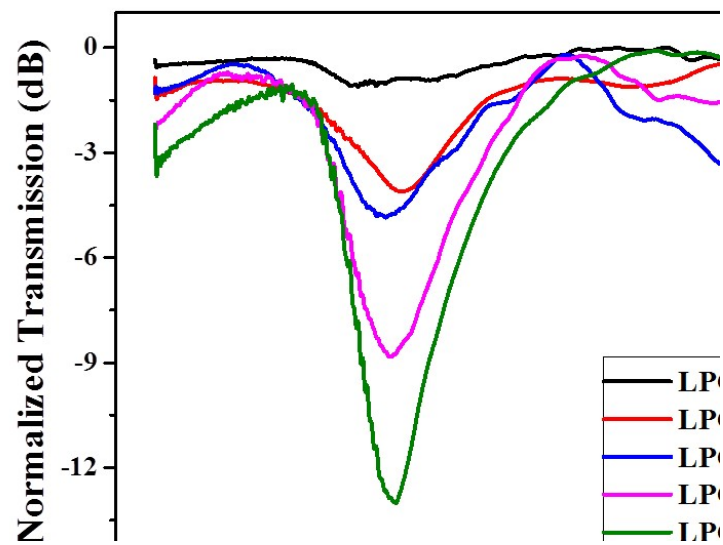


Figure 4. Measured transmission spectra of the PAA-LPGs with different lateral widths of PAA micropads.

Since LPG-1:1-600 has the highest signal-to-noise ratio, it was chosen for testing pH responses in the experiments. **Figure 5** (a) shows the measured responses of LPG-1:1-600 sensor to different pH solutions. The central resonant wavelength of the sensor shifts to longer wavelength when the pH increases from 2 to 7. It is because swelling of PAA ionic hydrogel induces a decrease of its refractive index.^[1d, 1g-1i] Consequently, the effective refractive index

of the fiber cladding mode becomes lower as it depends on the surrounding PAA ionic hydrogel via evanescent field. Therefore, a red-shift of the resonant wavelength occurred due to the increase in the difference of effective refractive index between the fundamental guided mode and the fiber cladding mode.^[16] At the same time, a weaker resonant peak was also observed, as shown in the inset of Figure 5 (a). It indicates that the swelling of PAA micropads reduces the strain applied on the microfiber and thus induces a decline of mode coupling strength. The measured sensitivity of the LPG pH sensor is 7.5 nm/pH, which surpasses significantly other reported LPG pH sensors.^[17] Since the resolution of the OSA

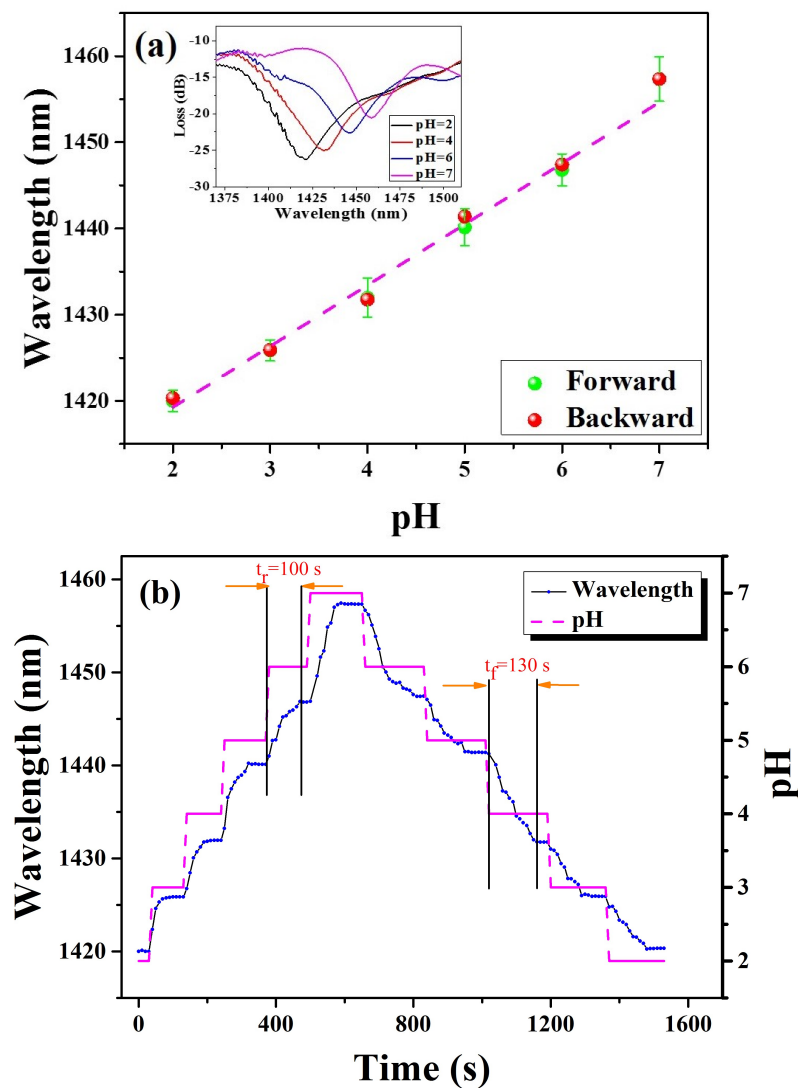


Figure 5. (a) Reversible shift of the dip wavelength of LPG-1:1-600 sensor with increasing and decreasing pH (the error bar is given based on the test of three sensors); (b) dynamic response of LPG-1:1-600 sensor to different pH solutions.

used in the experiment is 0.02 nm, the distinguishable pH change of the sensor is estimated as 0.0027.

The dynamic response of LPG-1:1-600 sensor to pH changes is shown in Figure 5(b). The OSA keeps sweeping with the period of 10 s during the measurement. In order to achieve a consistent measurement data, the PAA-LPG sensor has been pre-immersed into DI water before test. The measured response times of the sensor for increasing and decreasing pH processes are 100 s and 130 s, respectively, which are comparable with other reported fiber-optic pH sensors.^[18]

In summary, a new optical maskless stereolithography technology has been demonstrated to rapidly fabricate PAA ionic hydrogel micropatterns. Various 2D and 3D complex PAA microstructures with different feature sizes have been fabricated to show the versatility of the microfabrication technology. Particularly, PAA ionic hydrogel has been *in-situ* patterned into periodic micropads along a tapered optical microfiber to form a PAA-LPG sensor, which showed both very high sensitivity and fast response time in pH sensing. It is believed that the demonstrated micropatterning approach will trigger innovations in micro-engineering of PAA ionic hydrogels ranging from sensing to bio-functional devices.

Experimental Section

Materials:

Acrylic acid (anhydrous, contains 180-200 ppm MEHQ as inhibitor, 99%), 2-hydroxy-4'-(2-hydroxyethoxy)-2-methylpropiophenone (Irgacure 2959) and isopropanol (IPA) were purchased from Aldrich. Hydrochloric acid (HCl) and potassium hydroxide (KOH) are all analytical reagents. Deionized (DI) water with a resistance of 18 M Ω cm was used in all experiments.

Fabrication of PAA microstructures:

Photoinitiator (Irgacure 2959) was dissolved into AA solution with a concentration of 10 wt%. The solutions were first prepolymerized in the oven at the temperature of 100 °C for 5 minutes. Then, an own-established OMsL setup as shown in Figure S1 (a) and (b) was used for micropatterning process. With a spacer, a cover glass was placed upon the AA solution that was dropped on another glass slide. UV light will penetrate the cover glass and photopolymerize AA on the bottom side of the cover glass. The pre-designed microstructures were converted into own-defined image data and then loaded onto the DMD chip for generation of optical patterns. UV light source (365 nm) was used in the OMsL setup for photopolymerization of AA solutions. The intensities of UV light for 2D and 3D microstructure patterning are 103.12 mW/cm² and 51.56 mW/cm², respectively. The total exposure time is around 5 to 30 s. The exposed micropatterns were developed by using DI water and IPA, sequentially.

Fabrication of PAA-LPG pH sensors:

Standard single-mode optical fiber (SMF-28e, Corning) was used to prepare optical microfiber. A commercial fiber tapering machine (LZM-100, Fujikura Ltd., Japan) was utilized to taper the standard optical fiber with diameter of 125 μm into a microfiber with diameter of 30 μm. The length of the uniform taper waist is around 20 mm.

After mounting the microfiber on a glass slide, the prepolymerized AA solution was dropped on the glass slide to immerse the microfiber. The microfiber mounted glass slide was then placed on the sample stage of the OMsL system for optical exposure process, as shown in Figure S1 (c). PAA micropads were then periodically fabricated on the cover glass and encapsulated the microfiber through optical maskless projection exposure and pattern stitching techniques. The time used for single-image exposure in PAA-LPG fabrication is 10 s. The intensity of UV light (at the wavelength of 365 nm) used for exposure is 395.3 mW/cm².

Supporting Information

Supporting informations (including the microscopic images of PAA micropatterns with detailed information, the microscopic image and spectral responses of an LPG-3:7-1000 sensor) are available from the Wiley Online Library or from the author.

Acknowledgements

This work was partially supported by Hong Kong RGC GRF (Grant No.: PolyU 152211/14E) and PolyU Departmental General Research Fund (Project Code: 4-ZZBE).

References

- [1] a) B. Ghosh, M.W. Urban *Science* **2009**, *323*, 1458; b) D. Wandera, S.R. Wickramasinghe, S.M. Husson *J. Membr. Sci.* **2010**, *357*, 6; c) M.A.C. Stuart, W.T.S. Huck, J. Genzer, M. Muller, C. Ober, M. Stamm, G.B. Sukhorukov, I. Szleifer, V.V. Tsukruk, M. Urban, F. Winnik, S. Zauscher, I. Luzinov, S. Minko *Nat. Mater.* **2010**, *9*, 101; d) Q. Zhao, M. Yin, A.P. Zhang, S. Prescher, M. Antonietti, J. Yuan *J. Am. Chem. Soc.* **2013**, *135*, 5549; e) Q. Zhao, J.W.C. Dunlop, X. Qiu, F. Huang, Z. Zhang, J. Heyda, J. Dzubiella, M. Antonietti, J. Yuan *Nat. Commun.* **2014**, *5*; f) C. Zhao, S. Nie, M. Tang, S. Sun *Prog. Polym. Sci.* **2011**, *36*, 1499; g) M.J. Yin, C. Wu, L.Y. Shao, W.K.E. Chan, A.P. Zhang, C. Lu, H.Y. Tam *Analyst* **2013**, *138*, 1988; h) M.J. Yin, B.B. Gu, Q.A. Zhao, J.W. Qian, A. Zhang, Q.F. An, S.L. He *Anal. Bioanal. Chem.* **2011**, *399*, 3623; i) M.J. Yin, B.B. Gu, J.W. Qian, A.P. Zhang, Q.F. An, S.L. He *Anal. Methods* **2012**, *4*, 1292; j) Z. Gui, J. Qian, M. Yin, Q. An, B. Gu, A. Zhang *J. Mater. Chem.* **2010**, *20*, 7754; k) F. Zhou, P.M. Biesheuvel, E.-Y. Choi, W. Shu, R. Poetes, U. Steiner, W.T.S. Huck *Nano Lett.* **2008**, *8*, 725; l) A. Sidorenko, T. Krupenkin, A. Taylor, P. Fratzl, J. Aizenberg *Science* **2007**, *315*, 487; m) M. Ma, L. Guo, D.G. Anderson, R. Langer *Science* **2013**, *339*, 186; n) T. TANAKA, I. NISHIO, S.-T. SUN, S. UENO-NISHIO *Science* **1982**, *218*, 467; o) H. Li, J. Chen, K.Y. Lam *Biomacromolecules* **2006**, *7*, 1951.
- [2] a) B. Gu, M.-J. Yin, A.P. Zhang, J.-W. Qian, S. He *Sens. Actuators, B* **2011**, *160*, 1174; b) D. Buenger, F. Topuz, J. Groll *Prog. Polym. Sci.* **2012**, *37*, 1678; c) R.M. Rasal, D.E. Hirt *Macromolecular Bioscience* **2009**, *9*, 989; d) A.C. Pearson, M.R.

- Linford, J.N. Harb, R.C. Davis *Langmuir* **2013**, *29*, 7433; e) E.N. Chiang, R. Dong, C.K. Ober, B.A. Baird *Langmuir* **2011**, *27*, 7016; f) A. George, J.E. ten Elshof *J. Mater. Chem.* **2012**, *22*, 9501; g) P. Akkahat, V.P. Hoven *Colloids Surf., B* **2011**, *86*, 198; h) I.-T. Hwang, M.-S. Oh, C.-H. Jung, J.-H. Choi *Biotechnol Lett* **2014**, *36*, 2135; i) R. Dong, S. Krishnan, B.A. Baird, M. Lindau, C.K. Ober *Biomacromolecules* **2007**, *8*, 3082; j) Y.-M. Wang, Y. Cui, Z.-Q. Cheng, L.-S. Song, Z.-Y. Wang, B.-H. Han, J.-S. Zhu *Applied Surface Science* **2013**, *266*, 313; k) L. Herlogsson, Y.-Y. Noh, N. Zhao, X. Crispin, H. Siringhaus, M. Berggren *Adv. Mater.* **2008**, *20*, 4708; l) L. Herlogsson, X. Crispin, N.D. Robinson, M. Sandberg, O.J. Hagel, G. Gustafsson, M. Berggren *Adv. Mater.* **2007**, *19*, 97; m) S. Naficy, G.M. Spinks, G.G. Wallace *ACS Appl. Mater. Interfaces* **2014**, *6*, 4109; n) L.M. Dumitru, K. Manoli, M. Magliulo, L. Sabbatini, G. Palazzo, L. Torsi *ACS Appl. Mater. Interfaces* **2013**, *5*, 10819; o) K. Braam, V. Subramanian *Adv. Mater.* **2015**, *27*, 689.
- [3] a) M.R. Islam, Z.Z. Lu, X. Li, A.K. Sarker, L. Hu, P. Choi, X. Li, N. Hakobyan, M.J. Serpe *Anal. Chim. Acta.* **2013**, *789*, 17; b) J. Hu, G. Zhang, S. Liu *Chem. Soc. Rev.* **2012**, *41*, 5933.
- [4] M.C. Berg, J. Choi, P.T. Hammond, M.F. Rubner *Langmuir* **2003**, *19*, 2231.
- [5] A. Winkleman, R. Perez-Castillejos, M. Lahav, M. Narovlyansky, L.N.J. Rodriguez, G.M. Whitesides *Soft Matter* **2007**, *3*, 108.
- [6] G. Wu, Y. Xia, S. Yang *Soft Matter* **2014**, *10*, 1392.
- [7] Y. Mi, Y. Chan, D. Trau, P. Huang, E. Chen *Polymer* **2006**, *47*, 5124.
- [8] X. Chen, J. Sun, J. Shen *Langmuir* **2009**, *25*, 3316.
- [9] H.-W. Chien, T.-Y. Chang, W.-B. Tsai *Biomaterials* **2009**, *30*, 2209.
- [10] a) Y. Shen, Y. Liu, G. Zhu, H. Fang, Y. Huang, X. Jiang, Z.L. Wang *Nanoscale* **2013**, *5*, 527; b) J. Torgersen, X.-H. Qin, Z. Li, A. Ovsianikov, R. Liska, J. Stampfl *Adv. Funct. Mater.* **2013**, *23*, 4542; c) N. Annabi, A. Tamayol, J.A. Uquillas, M. Akbari, L.E. Bertassoni, C. Cha, G. Camci-Unal, M.R. Dokmeci, N.A. Peppas, A. Khademhosseini *Adv. Mater.* **2014**, *26*, 85; d) P. Zorlutuna, N. Annabi, G. Camci-Unal, M. Nikkhah, J.M. Cha, J.W. Nichol, A. Manbachi, H. Bae, S. Chen, A. Khademhosseini *Adv. Mater.* **2012**, *24*, 1782.
- [11] A.P. Zhang, X. Qu, P. Soman, K.C. Hribar, J.W. Lee, S. Chen, S. He *Adv. Mater.* **2012**, *24*, 4266.

- [12] M. Tanabe, G.W.M. Vandermeulen, W.Y. Chan, P.W. Cyr, L. Vanderark, D.A. Rider, I. Manners *Nat. Mater.* **2006**, *5*, 467.
- [13] a) V.V. Vasilevskaya, I.I. Potemkin, A.R. Khokhlov *Langmuir* **1999**, *15*, 7918; b) D. Klinger, K. Landfester *Macromolecules* **2011**, *44*, 9758.
- [14] C.C. Chiang, L.R. Tsai *Opt. Lett.* **2012**, *37*, 193.
- [15] W.J. Stephen, P.T. Ralph *Measurement Science and Technology* **2003**, *14*, R49.
- [16] T.W. MacDougall, S. Pilevar, C.W. Haggans, M.A. Jackson *Photonics Technology Letters, IEEE* **1998**, *10*, 1449.
- [17] a) F. Tian, J. Kanka, S.A. Sukhishvili, H. Du *Opt. Lett.* **2012**, *37*, 4299; b) J.-C. Mau, G.-R. Lin, M.-Y. Fu, W.-F. Liu *Microw. Opt. Techn. Let.* **2013**, *55*, 855.
- [18] a) A.B. Socorro, I. Del Villar, J.M. Corres, F.J. Arregui, I.R. Matias *Sens. Actuators, B* **2014**, *190*, 363; b) J.M. Corres, I. del Villar, I.R. Matias, F.J. Arregui *Opt. Lett.* **2007**, *32*, 29; c) Z.Q. Tou, C.C. Chan, J. Hong, S. Png, K.M.T. Eddie, T.A.H. Tan *BIOMEDO* **2014**, *19*, 047002.

Supporting Information

Rapid 3D Patterning of Poly(acrylic acid) Ionic Hydrogel for Miniature pH Sensors

Ming-jie Yin^a, Mian Yao^{a,b}, Shaorui Gao^a, A. Ping Zhang^{*a}, Hwa-yaw Tam^a, and Ping-kong A. Wai^b

[a] Mr. M. J. Yin, Mr. M. Yao, Dr. S. Gao, Dr. A. P. Zhang, Prof. H. Y. Tam
Photonics Research Center, Department of Electrical Engineering, The Hong Kong Polytechnic University, Hong Kong SAR, China
E-mail: azhang@polyu.edu.hk

[b] Mr. M. Yao, Prof. P. K. A. Wai
Photonics Research Center, Department of Electronic and Information Engineering, The Hong Kong Polytechnic University, Hong Kong SAR, China

3D microstructure measurement:

Microstructures of PAA hydrogels were measured by 3D laser scanning confocal microscope (VK-X200, KEYENCE, Japan). It is a non-contact laser scanning imaging machine. The magnification of lens used for scanning was 50 \times .

Swelling test:

PAA hydrogels were microfabricated with irradiation time of 5.0s, 7.5s, 10.0s, and 15.0s, respectively. The microstructures were immersed into different pH solutions, each was 2h. After equilibration, the mass of these samples was determined. The swelling degree was calculated from the ratio of the mass of the hydrogel in the swollen and dried states based on the average from two measurements.

Test of PAA-LPG pH sensors:

pH solutions were prepared by mixing of HCl and KOH solutions. The spectra of the LPG sensors were measured by using a broadband light source and optical spectrum analyzer (OSA) (AQ6370B, Yokogawa Ltd). The wavelength resolution of OSA was set to be 0.02 nm during the measurement. The sensor was immersed in DI water for 30 minutes before test in different pH solutions. The tests were conducted by dipping PAA-LPG sensors with different pH solutions.

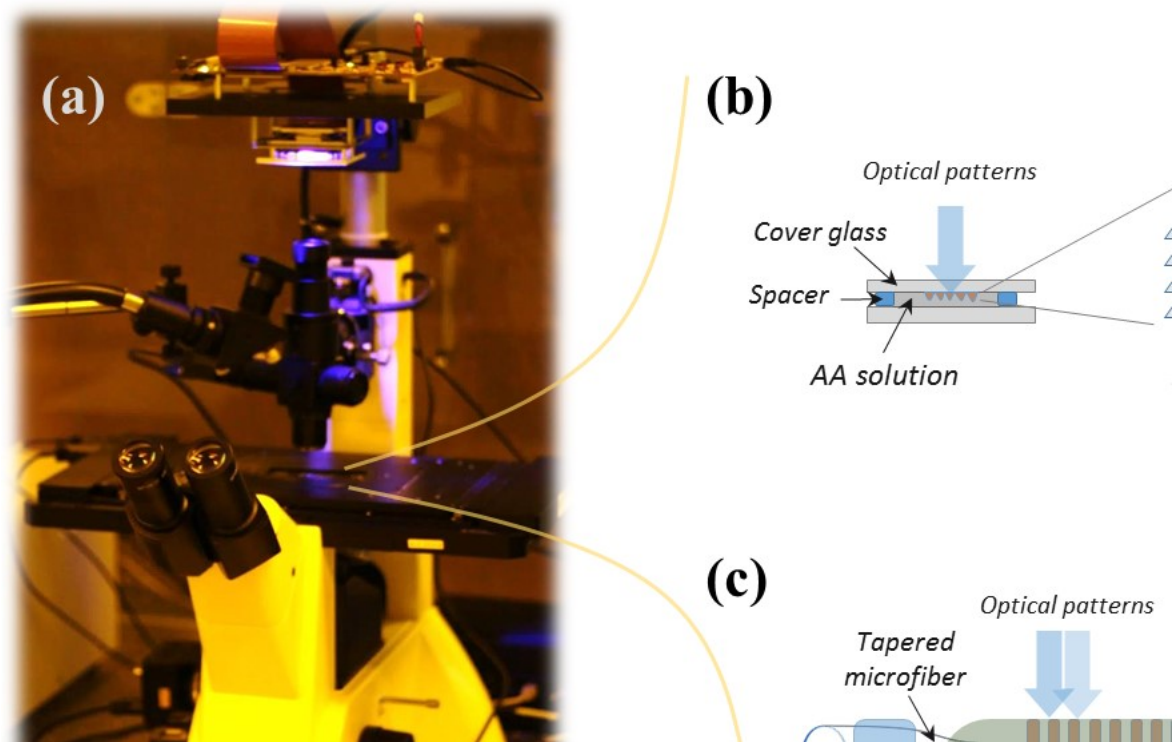


Figure S1. (a) Photo of the OMsL setup used for patterning PAA ionic hydrogel. (b) 3D microfabrication of PAA microstructures via layer-by-layer photopolymerization. (c) *In-situ* fabrication of periodic PAA micropads on an optical microfiber.

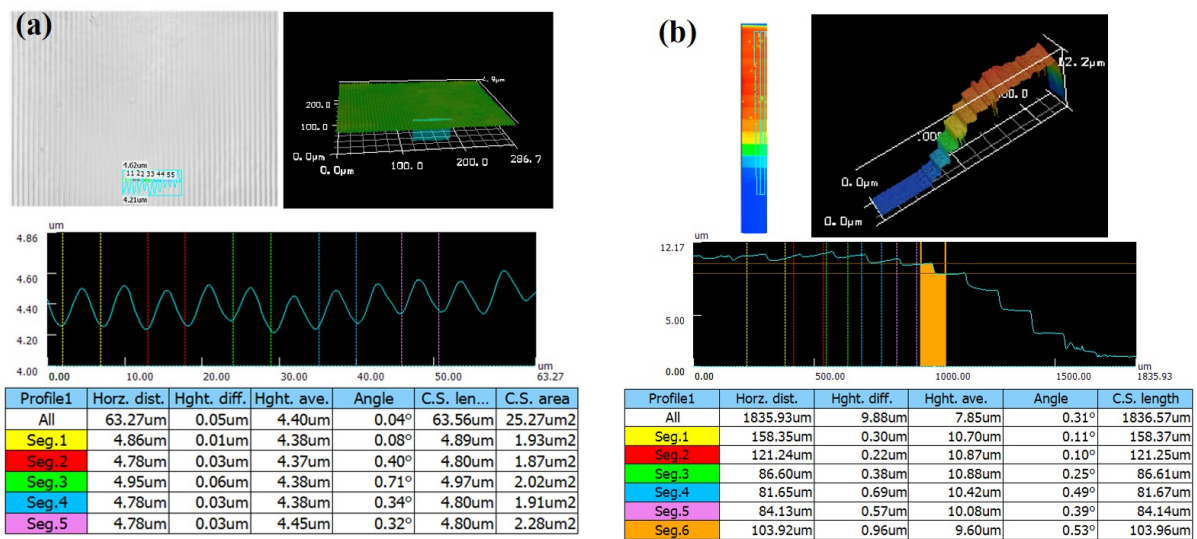


Figure S2. Images and profile parameters of the fabricated PAA gratings (a) and step-wise structures (b) for testing the lateral and depth resolutions of the platform (for patterning PAA ionic hydrogel), respectively. The images were measured by using 3D laser scanning confocal microscope.

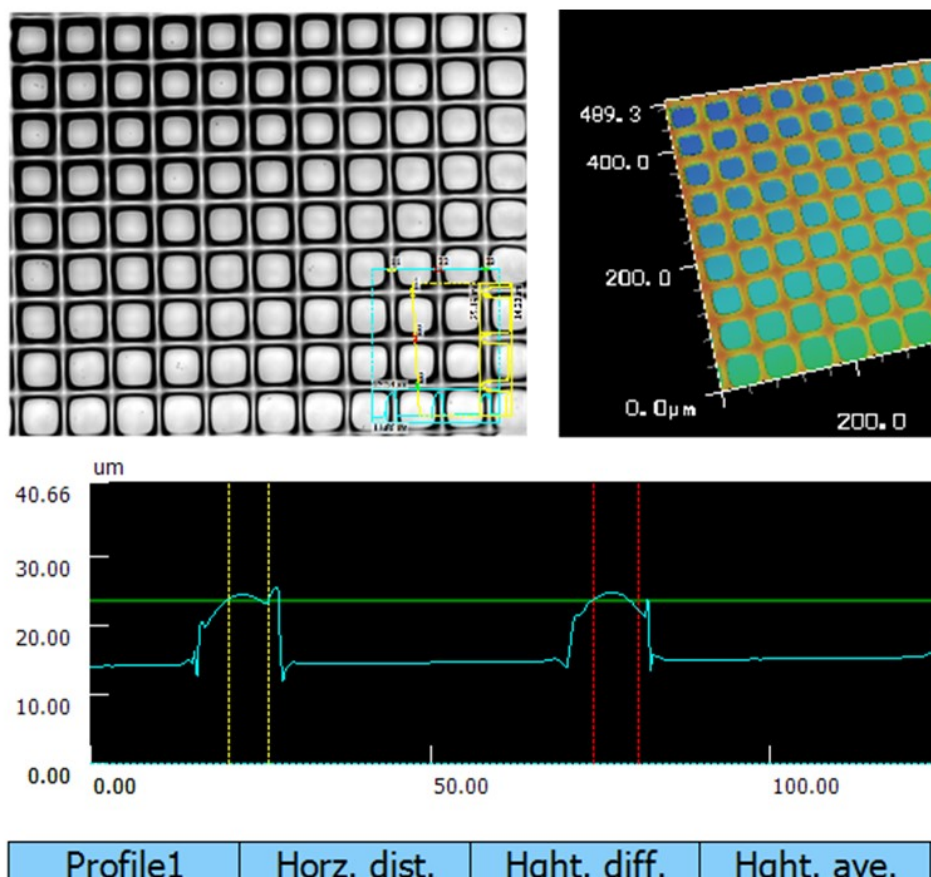


Figure S3. Images and line-width parameters of the PAA lattice grids measured by using 3D laser scanning confocal microscope.

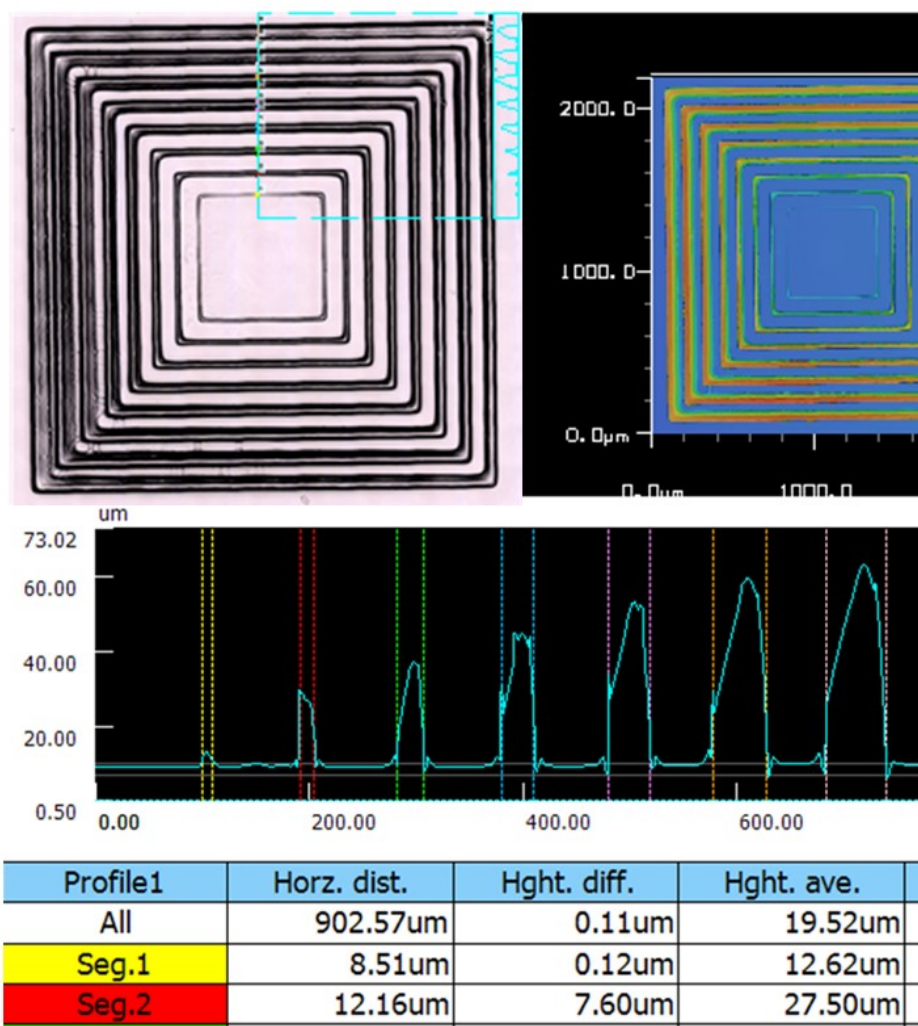


Figure S4. Images and line-width parameters of a concentric-square PAA micropattern measured by 3D laser scanning confocal microscope.

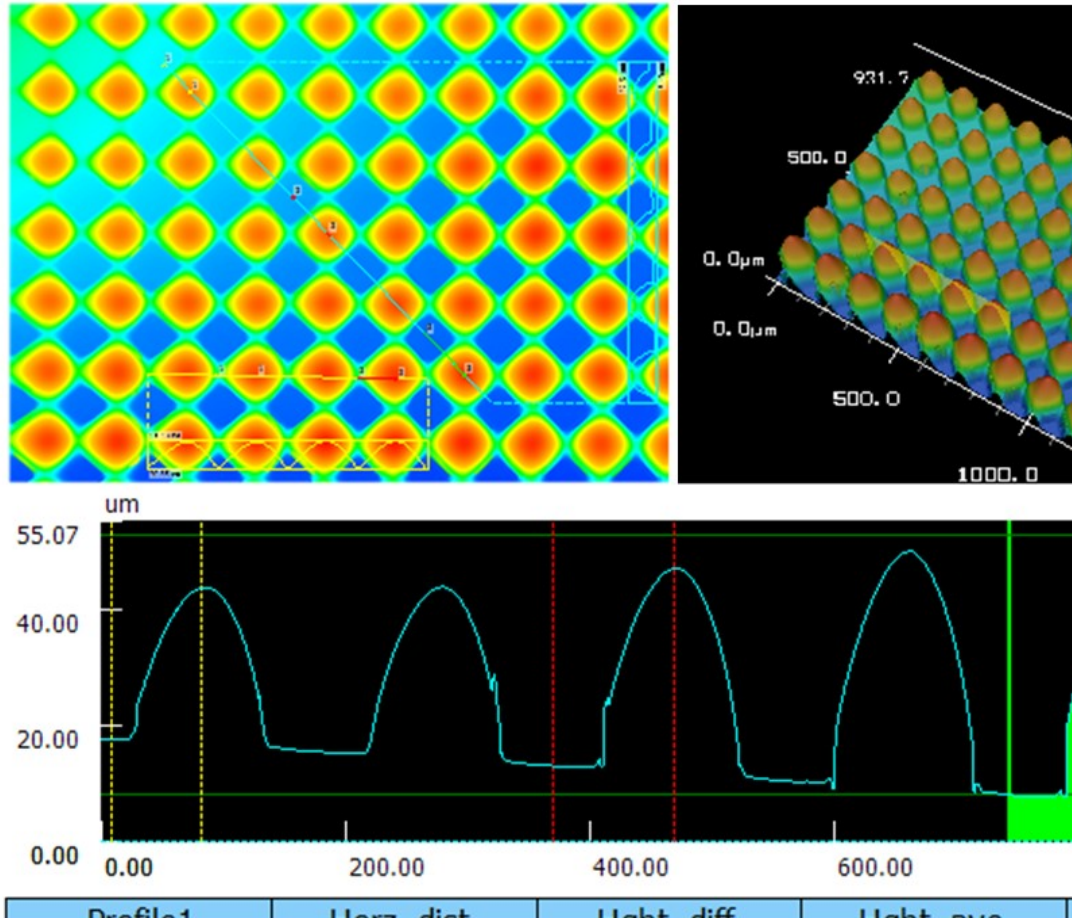


Figure S5. Images and profile parameters of the semispherical 3D microstructures measured by 3D laser scanning confocal microscope.

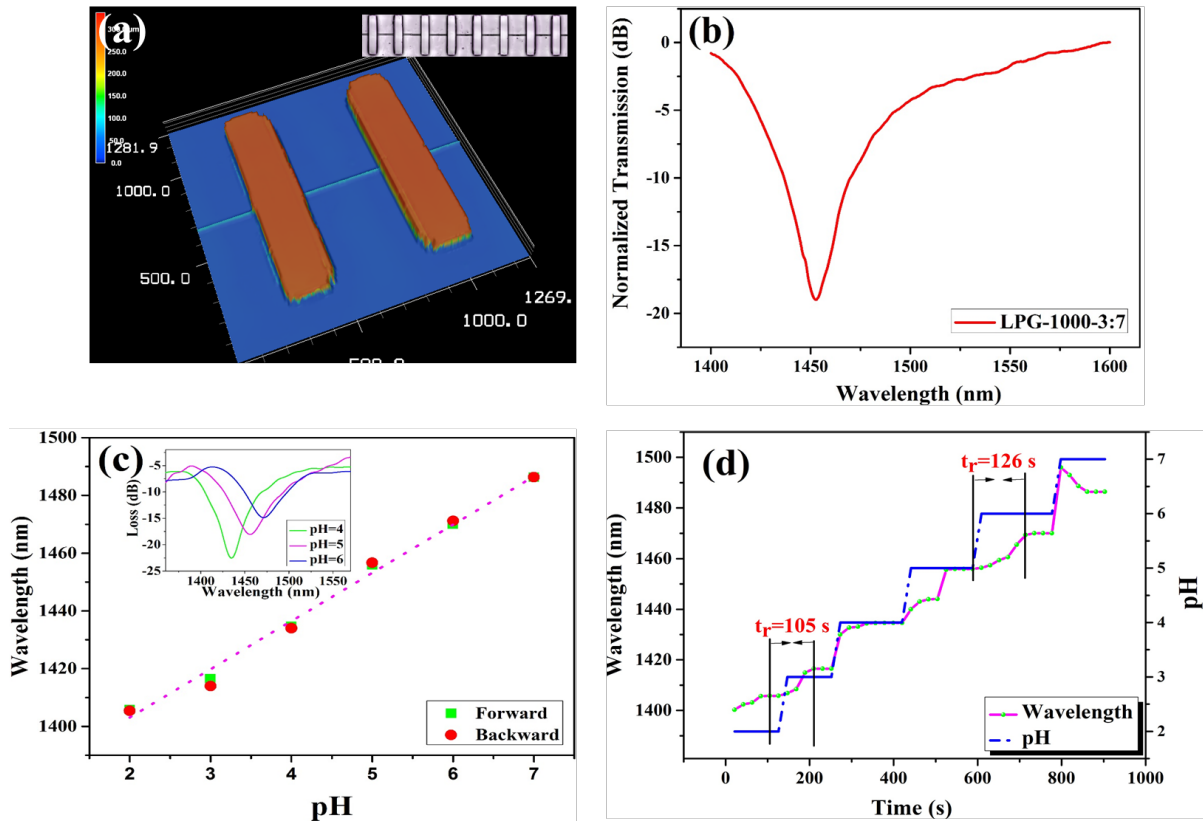


Figure S6. (a) Microscopic image of the PAA micropads of LPG-3:7-1000 sensor. (b) Measured transmission of the LPG sensor. (c) Wavelength shift of the sensor with pH change between 2 and 7. (d) Dynamic response of the pH sensor to different pH solutions. The sensitivity of the PAA-LPG sensor is 16.7 nm/pH, and the response time of the sensor is 120 s.